

Article

Multispectral Multibeam Echo Sounder Backscatter as a Tool for Improved Seafloor Characterization

Craig J. Brown ^{1,*} , Jonathan Beaudoin ², Mike Brissette ³ and Vicki Gazzola ¹

¹ Ivany Campus, Nova Scotia Community College, 80 Mawiomi Place, Dartmouth, NS B2Y 0A5, Canada; vicki.gazzola@nsc.ca

² Quality Positioning Services (QPS) Canada, Fredericton, NB E3B 1P9, Canada; beaudoin@qps.nl

³ R2Sonic, LLC, 5307 Industrial Oaks Blvd Suite 120, Austin, TX 78735, USA; mikeb@r2sonic.com

* Correspondence: craig.brown@nsc.ca

Received: 5 February 2019; Accepted: 7 March 2019; Published: 12 March 2019



Abstract: The establishment of multibeam echosounders (MBES), as a mainstream tool in ocean mapping, has facilitated integrative approaches towards nautical charting, benthic habitat mapping, and seafloor geotechnical surveys. The combined acoustic response of the seabed and the subsurface can vary with MBES operating frequency. At worst, this can make for difficulties in merging the results from different mapping systems or mapping campaigns. However, at best, having observations of the same seafloor at different acoustic wavelengths allows for increased discriminatory power in seabed classification and characterization efforts. Here, we present the results from trials of a multispectral multibeam system (R2Sonic 2026 MBES, manufactured by R2Sonic, LLC, Austin, TX, USA) in the Bedford Basin, Nova Scotia. In this system, the frequency can be modified on a ping-by-ping basis, which can provide multi-spectral acoustic measurements with a single pass of the survey platform. The surveys were conducted at three operating frequencies (100, 200, and 400 kHz), and the resulting backscatter mosaics revealed differences in parts of the survey area between the frequencies. Ground validation surveys using a combination of underwater video transects and benthic grab and core sampling confirmed that these differences were due to coarse, dredge spoil material underlying a surface cover of mud. These innovations offer tremendous potential for application in the area of seafloor geological and benthic habitat mapping.

Keywords: Multibeam; echo sounder; backscatter; multispectral; habitat mapping; surficial geology; Atlantic Canada

1. Introduction

The effective management of the earth's natural resources requires knowledge regarding the extent, geographical range, and ecological characteristics of the resource of interest—and maps are the pre-eminent means of recording and communicating this information. By combining these maps with spatial information on human activities, it is possible to accurately assess the compatibilities and conflicts between human use and the environment, and implement effective management strategies to mitigate any impacts [1]. On land, the development of aerial and satellite remote sensing technologies over the past few decades has increased the availability and affordability of electromagnetic remote sensed data in broad-scale terrestrial mapping, which in turn has dramatically improved our understanding of the spatial patterns and complexities of terrestrial ecosystems [2]. Multispectral satellite remote sensing, which acquires data from reflected light across a wide spectrum of electromagnetic wavelengths, has enabled scientists to develop classification routines to objectively map patterns of land cover and features (i.e., vegetation type, surface geology, man-made structures, etc.) [3]. Furthermore, by integrating this information with terrestrial digital elevation models (DEMs),

along with other environmental data sets (e.g., climate and surficial geology), sophisticated modelling of species distributions can be attained [2].

The limited penetration of electromagnetic radiation through seawater renders satellite and airborne remote sensing impractical for mapping the seafloor in all but the shallowest of waters. To map the ocean floor at a similar resolution to that achieved in terrestrial environments, we need to use other techniques, namely acoustic remote sensing. Multibeam echo sounders (MBES) have advanced to a level where we can now achieve high-resolution mapping of the seafloor at a similar spatial resolution as witnessed through the application of satellite and airborne optical remote sensing for mapping land [4–6]. Therefore, multibeam sonars have become a valuable tool for ocean floor mapping and, in addition to their wide scale use in the acquisition of bathymetric data for hydrographic charting, they are now commonly used for geological and benthic habitat mapping applications [6].

The *modus operandi* for producing surficial geology or benthic habitat maps has evolved in recent years, and it now routinely adopts the same types of objective segmentation/classification methods that are used for generating terrestrial maps from satellite remote sensed data sets [7]. Typically, the acoustic remote sensing data (e.g., MBES) are segmented into regions of similar characteristics (e.g., depths, terrain attributes, acoustic reflectance), which are validated through in situ observations/sampling (e.g., underwater imagery, grab, or core samples) in order to generate a thematic map of the seafloor (Figure 1). A wide variety of spatial integration techniques have been successfully used in recent studies [7], with the choice of method often being influenced by the available data sets, data resolution, spatial scale of the study, and the end-use of the map (Figure 1).

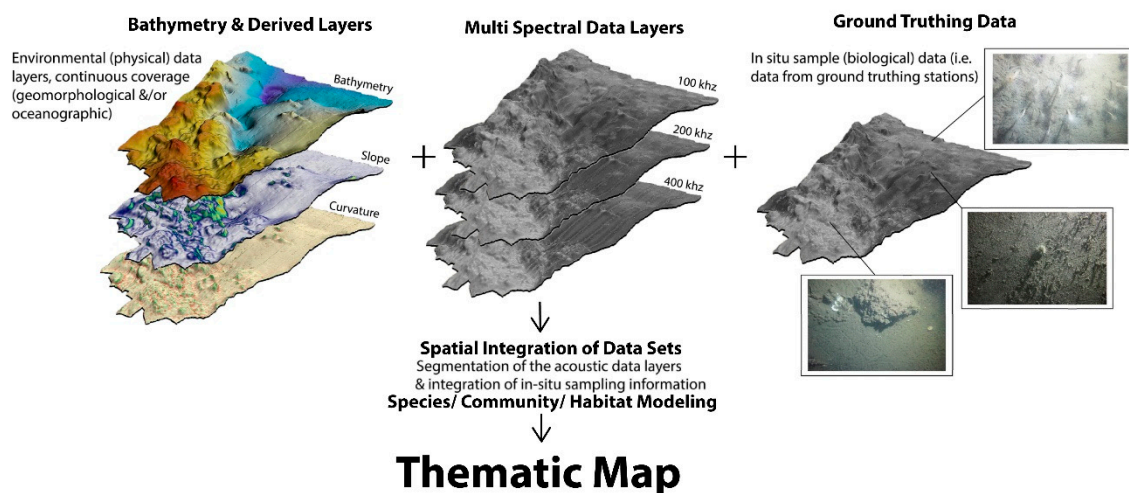


Figure 1. Generalized approach for the production of benthic habitat maps, illustrating typical data sets used for this type of application. The multispectral backscatter layers (i.e., multi-frequency) afforded by the R2Sonic system offer potential advantages over conventional, monochromatic (i.e., single-frequency) systems for improved seafloor characterization.

Multibeam systems record measurements of water depth (bathymetry), from which a number of secondary data layers that provide information of seafloor morphology can be generated (e.g., seafloor slope, aspect, terrain variability, etc.). The combination of these terrain metrics is valuable in defining and segmenting seafloor geology and benthic habitat [8–10]. In addition, most MBES today provide a measurement of the received seabed backscatter intensity, which can provide information regarding the geologic materials on the seabed based on their acoustic properties [11,12]. Following the geometric and radiometric correction of the returning signal, seabed backscatter intensity can also be used to segment and classify the seafloor. However, most multibeam systems operate around a single frequency or around a narrow band of a central frequency (i.e., monochromatic) [12,13]. This is analogous to the collection of data from a single wavelength from an optical satellite system, which would limit the

resolvability of terrestrial land cover features when compared to collecting data over broad band or multiple, dispersed spectral bands.

Not surprisingly, interest has grown in exploring the value that multispectral backscatter could offer for the improved classification of seafloor geological and habitat characteristics. Recent studies, to date, have explored the use of paired complementary MBES systems that are deployed simultaneously on the same vessel to collect data at wavelengths separated by more than one octave [13], or from surveys that are conducted at the same time from different platforms over the same area [14–16]. Advances in MBES transducer technology have resulted in wider operating bandwidths, with some systems on the market now being capable of spanning several hundred kHz to offer improved range resolution for bathymetric data collection [12]. However, to date, most of these systems only operate at a single frequency (or around a very narrow band of frequencies) at any one time, and therefore the acquired backscatter is still monochromatic in nature.

In 2016, the sonar manufacturer R2Sonic LLC. implemented new capabilities in their broadband MBES echo sounders, allowing for the operating frequency to be modified on a ping-by-ping basis. This offered, for the first time, the capability of simultaneously collecting multispectral backscatter data from a single MBES system. In this paper, we present the results from the first field trials of this system in the Bedford Basin, Nova Scotia, Canada, collecting data from three different frequencies (100, 200, and 400 kHz). The operating frequencies were unraveled in post processing, and the data sets were extensively groundtruthed using a combination of underwater imagery and sediment sampling using grab and core samplers to validate surficial sediment characteristics. We demonstrate the significant advantages that this can offer for improved seafloor characterization, and discuss what benefits this may afford the field of seafloor geological and benthic habitat mapping.

2. Materials and Methods

2.1. Study Area

Two multibeam sonar surveys were conducted in the Bedford Basin, Halifax, Nova Scotia over approximately the same area of seafloor at the mouth of the basin (Figure 2) in water depths of between 15–70 m. The survey area was selected, as it was known from previous multibeam surveys that were conducted by the Canadian Hydrographic Service (CHS) and the Geological Survey of Canada (GSC) to comprise a range of sediment types, ranging from bedrock through to silt with some differences in sediment stratigraphy [14,17]. Fader and Miller [17] describe features in the Bedford Basin that are caused by the disposal of dredge spoil, visible from sidescan sonar data, which were typically characterized by their circular shape and acoustically rough, high-backscatter surfaces, and that were often clustered together. The same features were also visible in lower-frequency MBES backscatter data, but not in higher-frequency MBES data sets that were collected in the area [14]—suggesting that this site would make an ideal candidate for testing the new multispectral MBES capability for the current study.

The physiography of the Bedford Basin is also extensively described [17]. A shallow water ridge comprising bedrock and gravel, including boulder-sized clasts, is present at the mouth of the basin, at the juncture with the Halifax Harbour Narrows, in around 15 m water depth. A shallow bank (named Sherwood Ridge by Fader and Miller [17]) runs approximately east to west and it separates the shallow, hard seafloor in the south of the survey site, from the deeper, softer seafloor in the north of the survey site. The deep sections of the Bedford Basin exhibit curvilinear morphological depressions in a relatively flat seafloor, which are visible in the acquired multibeam (see Results). The oceanography of the Bedford Basin has resulted in the flocculation and settlement of soft sediment deposits, including the input of organic material from sewage disposal over recent decades [17].

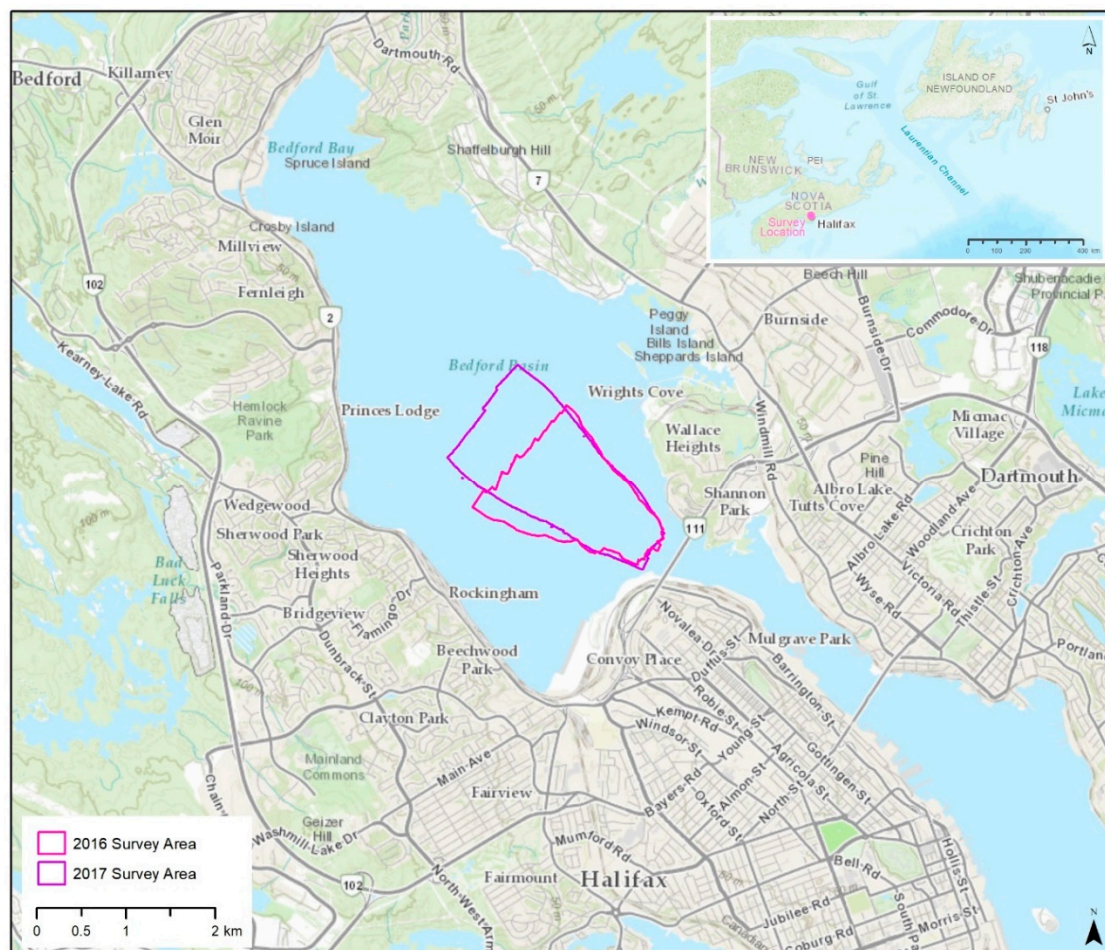


Figure 2. Overview map of the location of the 2016 and 2017 survey areas in the Bedford Basin, Nova Scotia, Canada.

2.2. Multibeam Sonar Data Acquisition

Two multibeam sonar surveys were conducted over the test area (Figure 2): 1) the first survey was conducted on 20 April 2016; and, 2) the second survey was conducted on 2 May 2017. For both of the surveys, an R2Sonic 2026 MBES was pole-mounted on the port side of the MV Eastcom, a 12 m fiberglass survey vessel. The transducer mount was fitted with a Valeport sound velocity probe and a POS MV Wave Master Inertial Navigation System (INS). The two Trimble GPS antennas from the INS were mounted on the bow of the survey platform, and all the systems integrated through the QPS QINSy software installed on the acquisition PC aboard the wheelhouse of the vessel. SVP casts at the time of survey were conducted using an AML Base X2 that was fitted with a set of conductivity, temperature, and pressure probes.

Survey lines were run in a NW-SE orientation with ~50% survey line overlap. The R2Sonic multibeam was configured to collect data at 100, 200, and 400 kHz operating frequencies on sequential pings, with operating settings that were tuned to achieve full coverage across these frequencies. The backscatter signal was monitored throughout acquisition using the R2Sonic saturation-monitoring tool to optimize data quality and avoid signal saturation.

Bathymetry and backscatter data were assessed during data acquisition to ensure data quality, and bathymetric post processing of the data was carried out using the QPS Qimera software suite. QPS FMGT software was used to process the multispectral backscatter data. CTD casts that were provided for each area/time period were used during post-processing to calculate absorption coefficients for frequency dependent attenuation of the transmit pulse to allow for correction

of the backscatter signal. The QPS FMGT software package enables frequency-specific pings to be unraveled from the multibeam datagram, and separate backscatter mosaics generated for each individual operating frequency (i.e., 100 kHz, 200 kHz, and 400 kHz) (Figure 3). This was the only frequency-specific radiometric correction that needed to be applied in FMGT, all other frequency-specific corrections pertaining to beam widths, etc, are automatically applied in FMGT. This results in the relative intensity (normalized) of the backscattered signal without the dependence of the beam's incidence angle in the output mosaic. The normalization is done by compiling an average angular response curve for a 300 ping rolling buffer and then normalizing the return signal of any given beam to a reference value in the angular range of 30–60 degrees (centered on 45 degrees). The port and starboard returns are separately averaged. The corrected mosaics for each frequency and from each data set were exported as 0.5 m ASCII x,y,bs intensity files for further comparison with ground truthing data sets in ArcGIS. Bathymetry data were manually cleaned for erroneous soundings in the QPS Qimera software package. Tidal corrections were applied while using observed tide data from the tide gauge at the Bedford Institute of Oceanography, which was directly adjacent to the study area. Bathymetric surfaces, backscatter mosaics, or each of the three operating frequencies for each of the two surveys are presented in Figures 4 and 5.

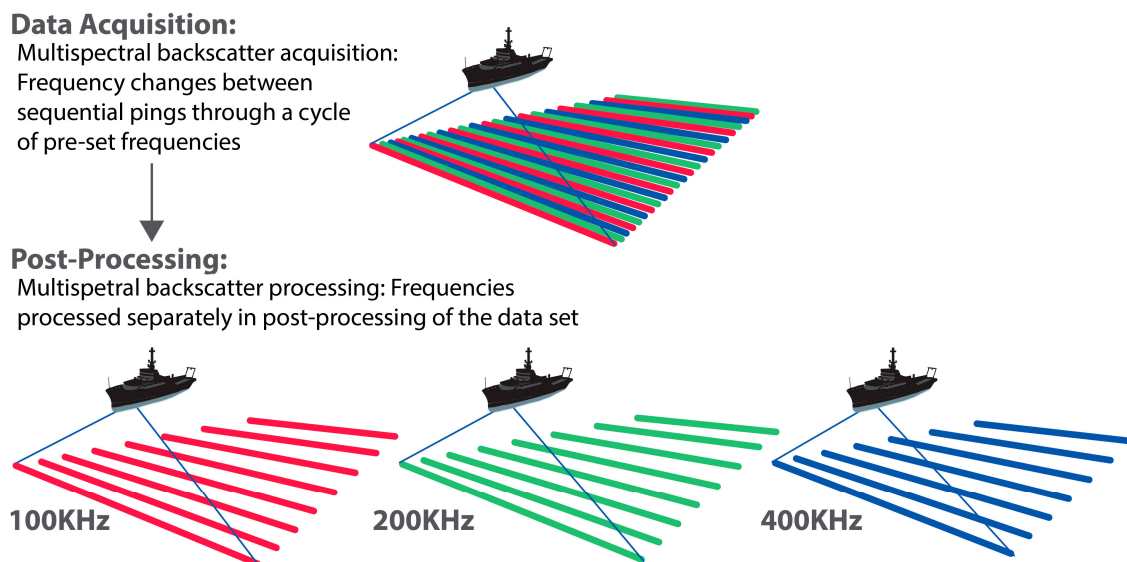


Figure 3. Data acquisition and post-processing of multispectral backscatter data.

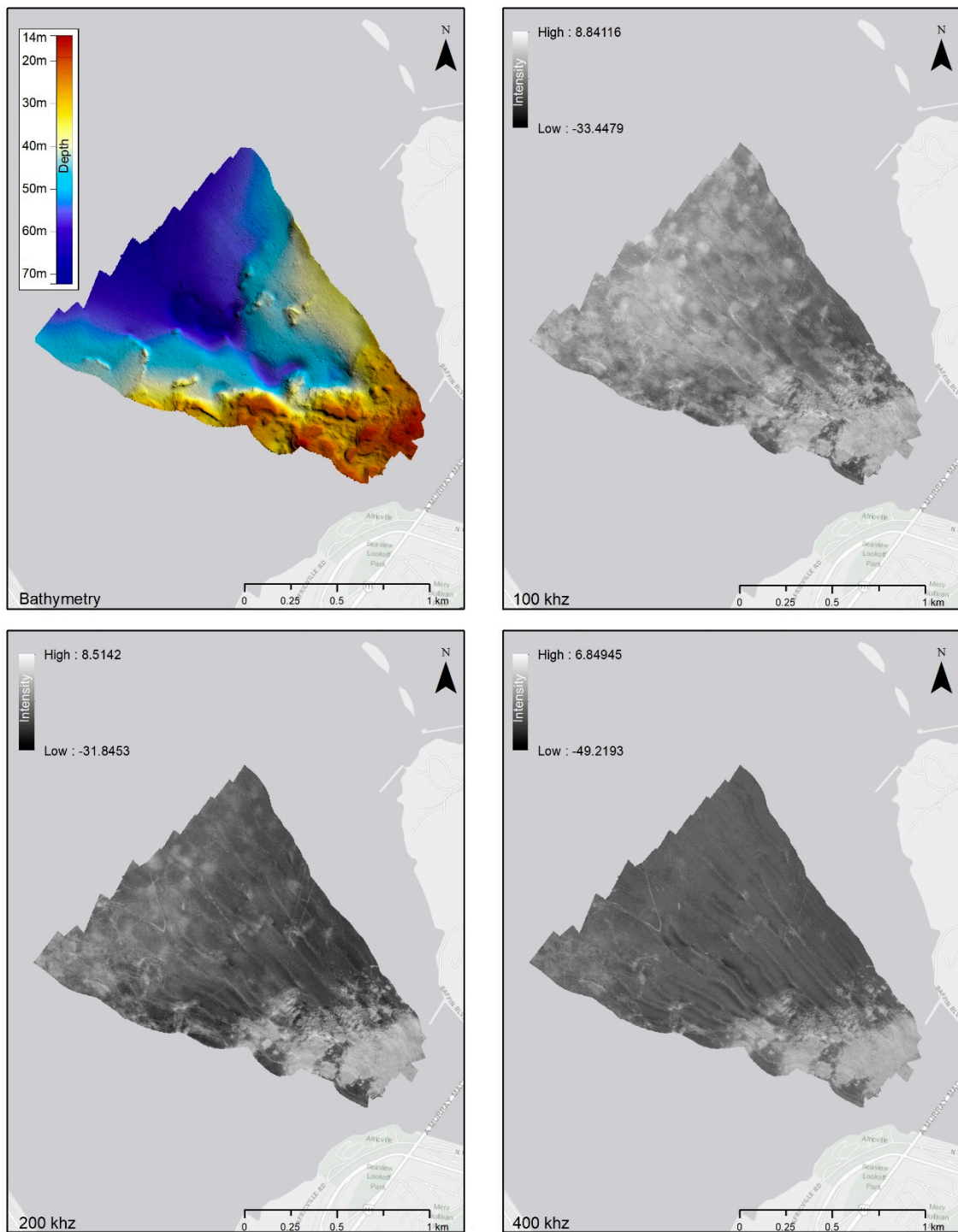


Figure 4. 2016 multibeam echosounders (MBES) bathymetry and multispectral backscatter: 100 kHz, 200 kHz, and 400 kHz mosaics.

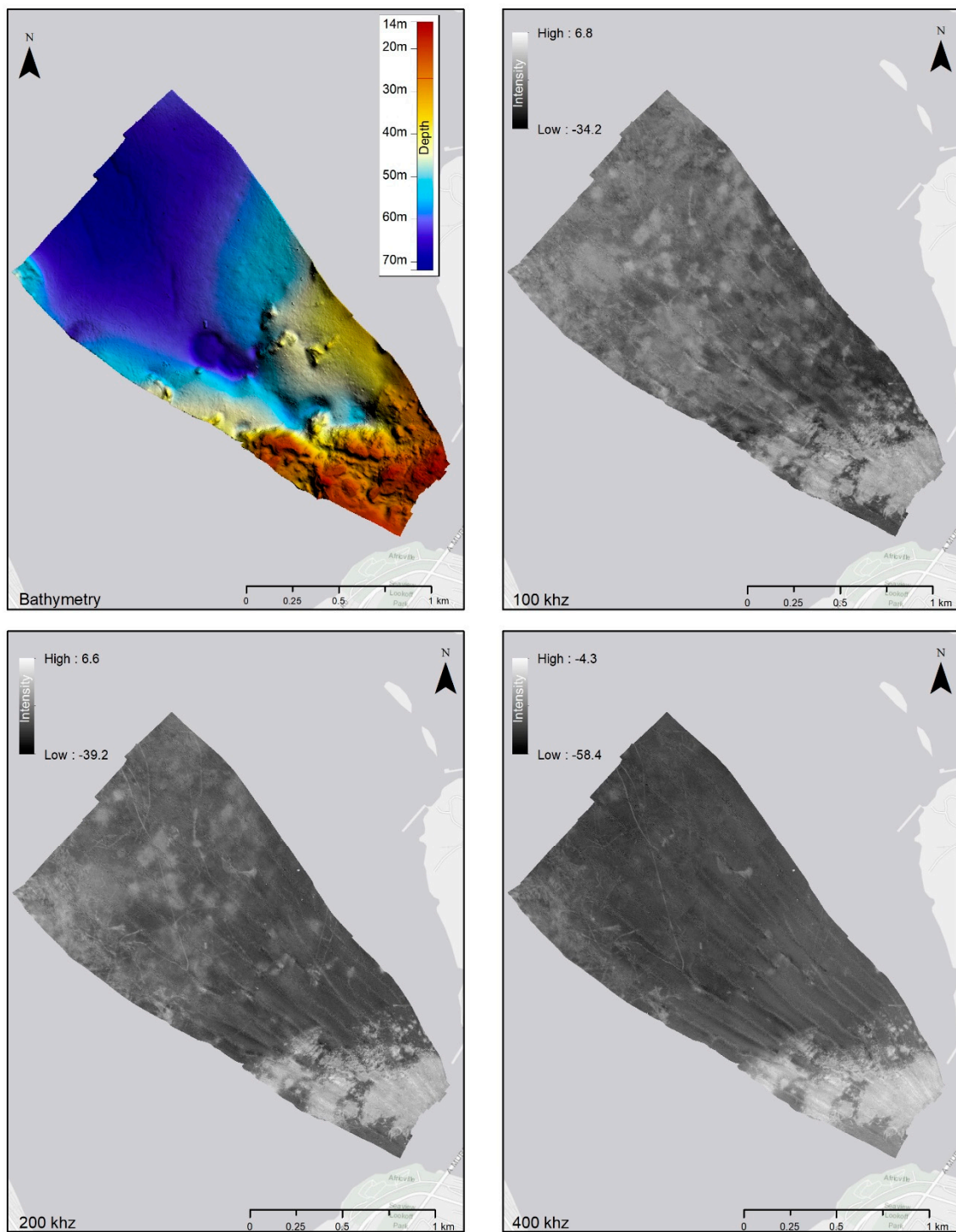


Figure 5. 2017 MBES bathymetry and multispectral backscatter: 100 kHz, 200 kHz, and 400 kHz mosaics.

2.3. Ground Validation Surveys

A variety of seafloor ground validation methods were used to quantify the seafloor sediment characteristics over the study area during a number of different surveys from the MV Eastcom. Georeferenced seafloor photographs were collected within the survey area in March 2016 using a drop-down underwater camera that was frame fitted with a Sub-C underwater camera and lights. Further imaging surveys were conducted in March 2017 and November/December of 2018 using a 4k Panasonic GH4 camera system in subsea housing mounted on a tow frame and fitted with high-powered underwater lights. For all the camera surveys, the GPS vessel position

was recorded during deployments using the QPS QINSy navigation software. Positional accuracy was estimated to be approximately ± 5 m through matching changes in substrate boundaries and other targets (e.g., wrecks) visible on the video data to the same targets visible in the MBES data set (e.g., changes in backscatter in the Narrows). Positional data was exported and then used to georeference photograph/video data by linking the UTC time stamps between the video data and GPS data sets. The imagery data was separately classified into substrate classes for comparison with the MBES backscatter data. Table 1 summarizes the video/photographic data that was collected over the multiple surveys. Figure 6 presents the classified camera track data.

Table 1. Seafloor classes derived from visual analysis of the subsea video and photographic data sets.

Seafloor Class	Representative Seafloor Image	Description
Mud		Mud with signs of bioturbation. Burrowing anemones, tube worms and other invertebrates.
Cobbles and boulders with mud		Cobbles and boulders with extensive epifauna of barnacles, hydroids and coralline algae. Patches of mud, with signs of bioturbation, visible between coarser substrate.
Gravel, cobbles and boulders		Coarse, mixed substrate ranging from gravel through to large boulders/outcropping bedrock. Epifauna comprising barnacles, bryozoan, hydroids and other invertebrates. Scallops frequently observed. No visible fine sediments.

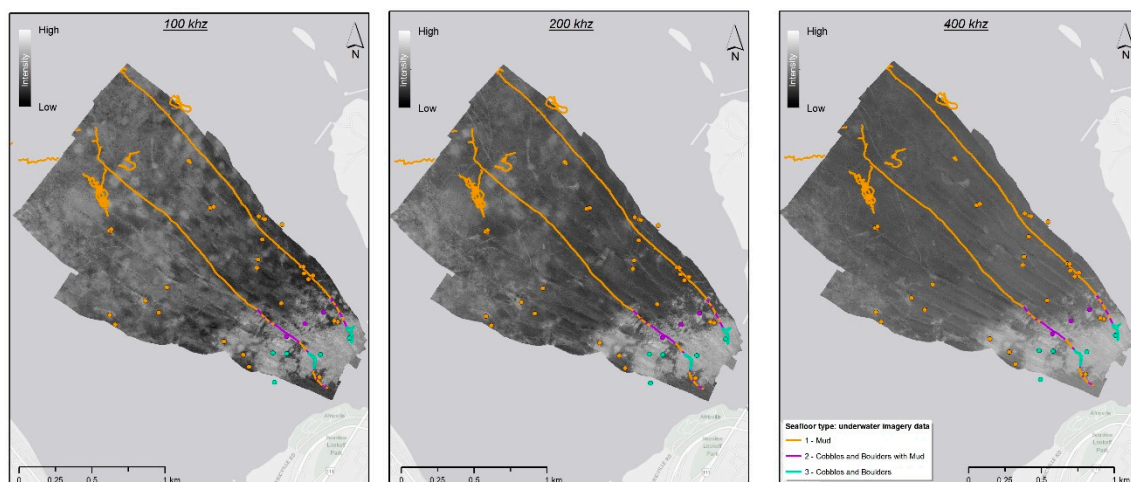


Figure 6. Classified video and photographic ground truthing data sets overlaid on a combined 2016 and 2017 100 kHz backscatter mosaic.

A total of 19 sediment grain size samples were collected using a 0.1 m² van veen grab sampler. The grab was deployed over the side of the vessel, and surficial sediment samples were recovered to the surface from the target location that was selected from the backscatter mosaics of areas of interest within the survey site. The position of each grab on the seafloor was recorded through a position fix while using QPS QINSy navigation software, so that the sediment characteristics from each grab could be compared against the MBES data sets. Positional accuracy of grab locations on the seafloor was estimated to be ±5 m. Each grab sample was photographed at the surface and a description of the sediment recorded. A subsample of the sediment from each grab was transferred from the sediment surface into a ziplock bag for sediment grain size analysis. A summary of the grab sample data sets is included in Table 2 and is shown in Figure 7.

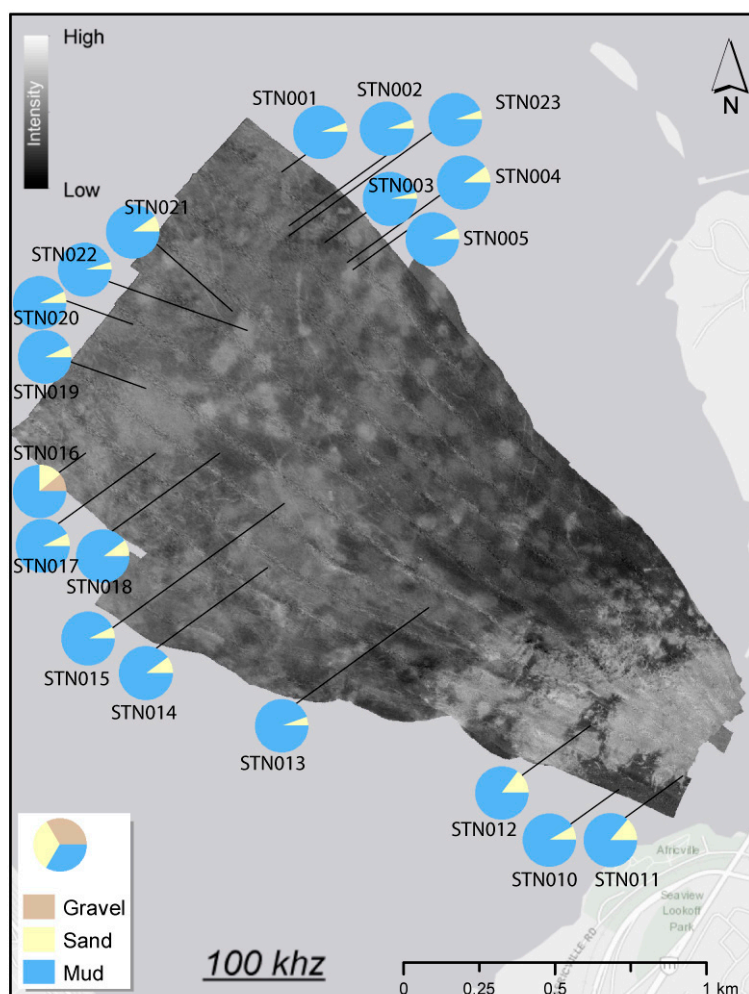


Figure 7. Sediment grain size data from van veen grab samples presented as percentage gravel, sand, and mud, overlaid on the 2017 100 kHz backscatter mosaic.

Table 2. Seafloor sediment information from the van veen grab samples.

Station	Percentage Grain Size		
	% Gravel	% Sand	% Mud
001	0	5	95
002	0	5	95
003	0	4	96
004	0	10	90
005	0	6	94
010	0	9	91

Table 2. Cont.

Station	Percentage Grain Size		
	% Gravel	% Sand	% Mud
011	1	14	85
012	0	15	85
013	0	5	95
014	1	10	89
015	0	7	93
016	11	14	75
017	0	7	93
018	0	10	90
019	0	7	93
020	0	7	93
021	0	5	95
022	0	10	90
023	0	6	94

Multicore samples were also conducted at a number of targeted sites where differences in backscatter were visible between the three MBES operating frequencies. The corer was lowered to the seafloor and the samples were retrieved to the surface. Core penetration depth was recorded and a photograph was taken of a representative core, and the representative samples were extruded for sediment grain size analysis. Where it was possible, subsamples were taken from the core sediment surface and from the bottom of the core at the maximum point of penetration. A summary of the sample data is presented in Table 3 and is shown in Figure 8.

Table 3. Seafloor sediment information from the multicore samples.

Station	Mean Maximum Depth of Core Penetration	Position of Sediment Sample from Core	Mean Percentage Grain Size			Description/Number of Cores for Grain Size Analysis
			% Gravel	% Sand	% Mud	
MC2	31 cm	Sediment surface	0.2	6	93.8	Soft mud; n = 3
		Bottom of core	0.8	6	93.2	Soft mud; n = 3
MC3	7.5 cm	Sediment surface	0.1	4.4	95.5	Soft mud; n = 2
		Bottom of core	0.4	1.7	97.9	Soft mud; n = 1
MC4	23 cm	Sediment surface	0	1.7	98.3	Soft mud; n = 2
		Bottom of core	0.1	2	97.9	Soft mud; n = 2
MC6	12 cm	Sediment surface	0.1	5	94.9	Soft mud; n = 2
MC7	29 cm	Sediment surface	0.1	5.9	94	Soft mud; n = 2
		Bottom of core	0	3.1	96.8	Soft mud; n = 2

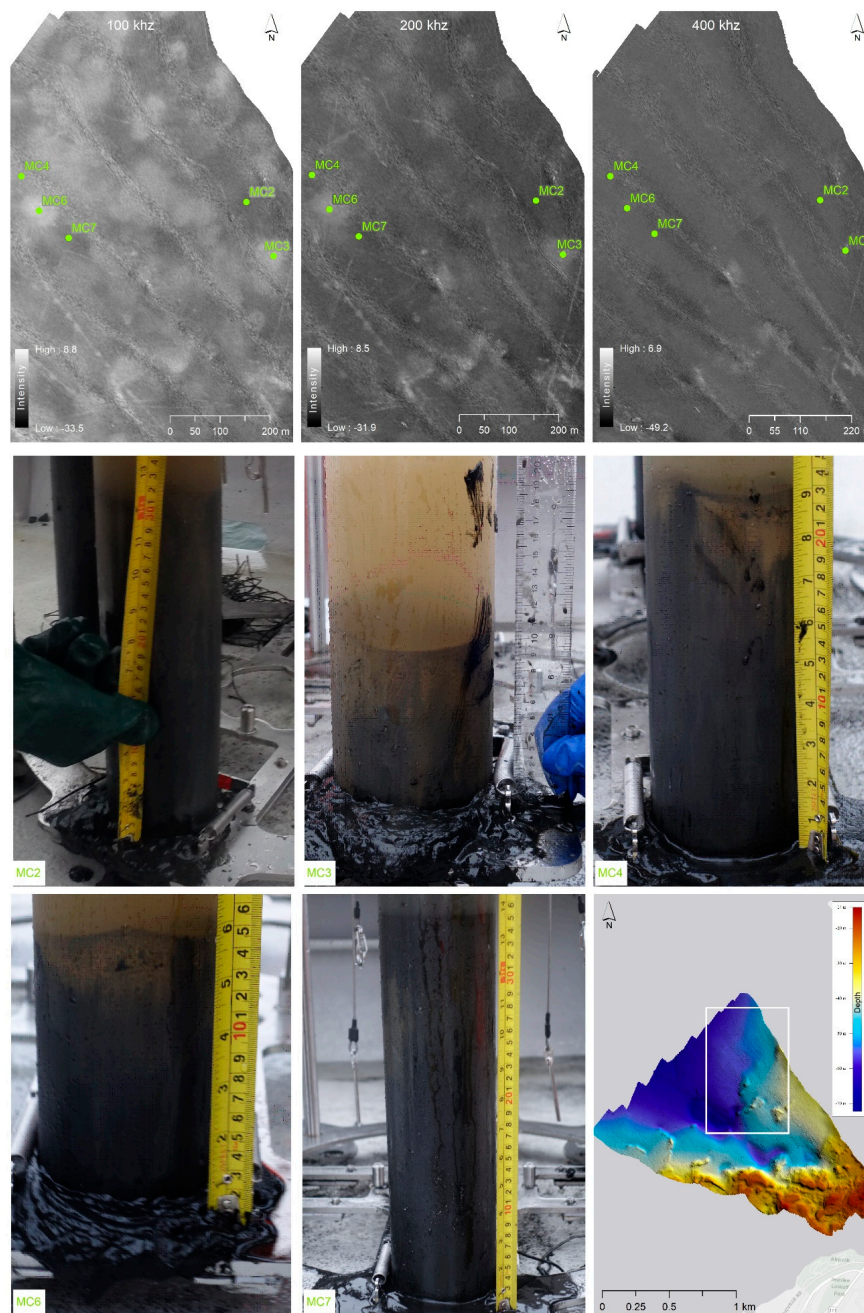


Figure 8. Example of benthic core samples from three adjacent sampling stations overlaid on the 2017 multispectral backscatter mosaics (100, 200, and 400k Hz). Differences in the backscatter intensities correspond to changes in core penetration depths, suggesting that the high intensity backscatter features visible in the lower frequency mosaics correspond to harder material (dredge spoil) beneath a surface covering of mud.

3. Results

The multispectral MBES test site covered an area of approximately 2 km² immediately to the north of the mouth of the basin. Bathymetry in the survey area that ranged from a minimum depth of 15 m in the SE of the site, to a maximum depth of 69 m in the centre of the basin (Figures 4 and 5). Within the survey area, the previously described seabed features are clearly visible. At the mouth of the basin, at the juncture with the Narrows, a shallow water ridge comprising bedrock and gravel, including boulder-sized clasts, was visible at around 15 m water depth. At all three operating frequencies, for both MBES surveys, high backscatter returns characterized this feature (Figures 4 and 5). A shallow

bank (named Sherwood Ridge by Fader and Miller [17]) is visible, running approximately east-west and separating the shallow, hard seafloor in the south of the survey site, from the deeper, softer seafloor in the north of the survey site (Figures 4 and 5).

The deep sections of the Bedford Basin exhibit curvilinear morphological depressions in a relatively flat seafloor (Figures 4 and 5). These deeper sections of the survey site to the north of Sherwood Ridge reveal differences in the backscatter intensities between the three operating frequencies. The 400 kHz data set reveals a predominant, relatively low, uniform backscatter return, with features that are consistent between the two temporal surveys (Figures 4 and 5). As the operating frequency decreases, circular patches of higher backscatter of various sizes (up to approximately 70 m diameter) become visible in the 200 kHz and 100 kHz mosaics. This is particularly apparent in the 100 kHz mosaic (Figures 4 and 5), suggesting a frequency dependent response of the seafloor that is caused by the surficial sediment characteristics. The same changes in intensity across the area were present in both the 2016 and 2017 data sets, suggesting that these features are stable and not subject to short-term changes in seafloor characteristics within the time frame of this study.

A comparison of the three multispectral mosaics within each of the surveys with the underwater imagery data collected using a drop-down camera systems confirmed that over most of the deeper-water regions of the study site the seafloor comprised of soft mud, which was colonized by various soft sediment biota (e.g., burrowing anemones, polychaete worms, etc.) (Figure 6 and Table 1). This corresponds with the uniform low backscatter returns of the 400 kHz mosaic, but not the patches of higher backscatter that were visible in the 100 and 200 kHz mosaics (Figures 4 and 5). In contrast, at the entrance to the Narrows, the seafloor comprised a mixture of coarse substrata (bedrock, boulders, and cobbles with attached epifauna) (Figure 6 and Table 1). The backscatter in this region aligned closely between the three multispectral mosaics, displaying high backscatter returns that are indicative of a hard seafloor (Figures 4 and 5). The underwater imagery data also revealed transitional areas in the proximity to the Narrows that were characterized by mixed substrata of coarse sediment (cobbles and boulders) interspersed with patches of mud (Figure 6 and Table 1).

The sediment grab samples from the survey site indicated that mud was the predominant sediment type at the surface of the seafloor over the vast majority of the survey area (Figure 7). Table 2 presents a summary of sediment grab samples. Examination of the sediment samples at the time of collection revealed that the surface of the sediment within each grab sample was well oxygenated, but it turned anoxic in nature within a few millimeters of the sediment-seawater interface, as indicated by the change in sediment colour and smell (Table 2 and Figure 7). Particle grain size analysis revealed that the mud fraction of the sediment (< 63 μm grain size) consisted of over 90% of the sample volume from all of the samples collected, with no detectable gravel within the surface sediment, except four sampling stations (stations 11, 12, 14, and 16) (Table 2 and Figure 7). At these four stations, the percentage of sand was higher and gravel was detected in stations 11, 14, and 16 (1%, 1%, and 11%, respectively). Station 16 and 14 coincided with high backscatter features on the 100 kHz mosaic, and station 11 from an area of low backscatter in the Narrows. It should also be noted that stations that showed no evidence of coarser sediments also coincided with the high backscatter features on the 100 kHz mosaic.

Sediment core samples collected at targeted sites both on and off the higher backscatter features visible in the 100 and 200 kHz mosaics revealed a difference in the depth of penetration of the cores. Samples collected within the high backscatter intensity features had lower core penetration into the substrate (e.g., station MC3 and MC6—Figure 8 and Table 3) compared with samples collected adjacent to these features where the backscatter was lower across the operating frequencies (e.g., MC2 and MC7—Figure 8 and Table 3). Grain size analysis revealed that the substrate collected by the corer comprised predominantly of mud (< 63 μm grain size), with little difference between top and bottom of the core. However, the depth in penetration likely indicates harder material preventing core penetration, which would not have been collected by the corer due to the inability of the core barrel to penetrate into coarse-grained sediment.

A comparison of the three multispectral mosaics along a transect from the mouth of the Bedford Basin to the deep water in the centre of the basin for each of the two surveys indicates where the backscatter intensities vary between the three operating frequencies (Figure 9). Patterns were similar for both the 2016 and 2017 data sets, although the absolute backscatter values between the surveys differed slightly due to the uncalibrated nature of the MBES systems [12]. Backscatter intensities in the mouth of the Bedford Basin at the three operating frequencies, which the underwater imagery confirmed as bedrock, cobbles, and gravel, were similarly high in intensity. The backscatter intensity between the three operating frequencies diverged in the deeper water, where the differences were visible across the three mosaics, even though the imagery data showed little difference in surficial sediment characteristics over the site (predominantly mud).

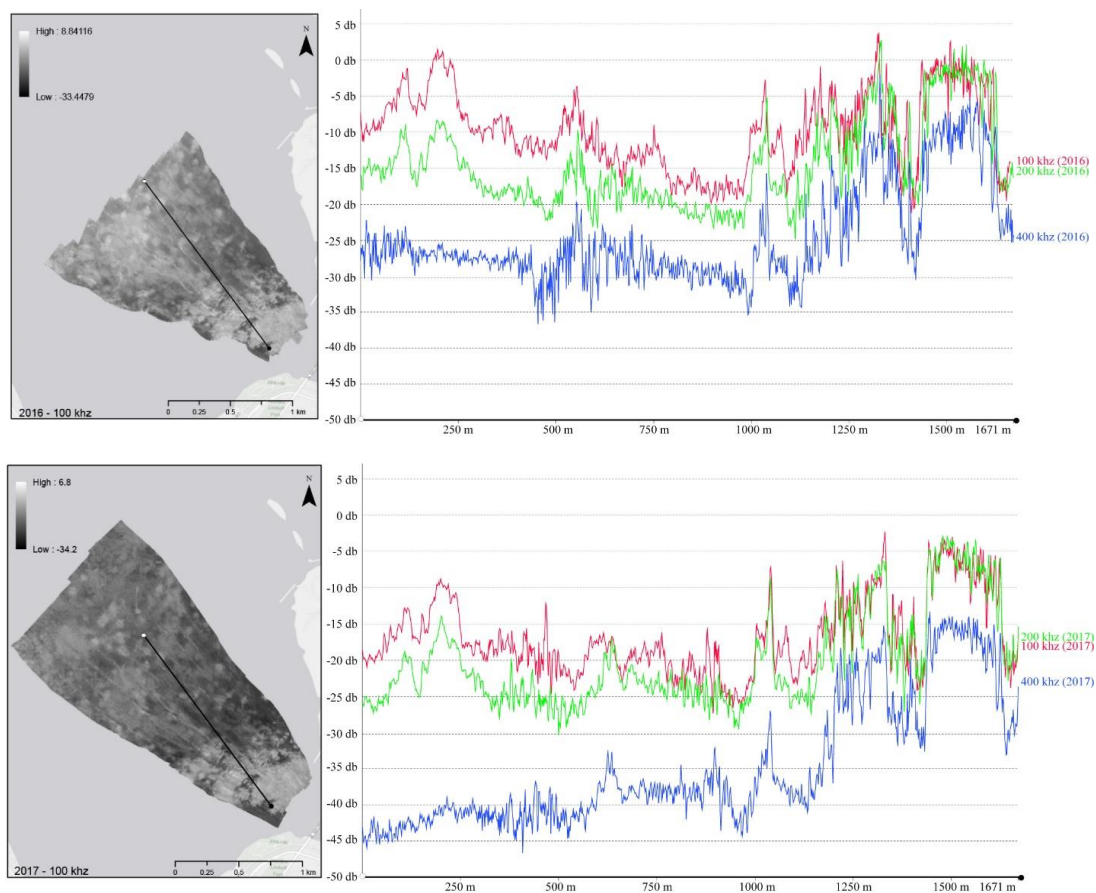


Figure 9. Top: 2016 data set. Bottom: 2017 data set. Comparison of differences in backscatter intensities within the survey site between the multispectral mosaics. Backscatter intensities from the three multispectral mosaics are compared along the transect shown on the 100 kHz mosaic (left). Backscatter intensities are similar in the hard-substrate region at the mouth of the narrows (SE of the site), and differences are visible in deeper water that is associated with the dredge spoil deposits.

4. Discussion

The physiography of the Bedford Basin that is revealed by this study is in agreement with earlier studies of this area [17]. The seafloor imagery and sediment sampling revealed that seafloor surficial sediments predominantly comprised of mud (Figures 6–8; Tables 1–3). The deep sections of the Bedford Basin exhibit curvilinear morphological depressions in a relatively flat seafloor (Figures 4 and 5). The 400 kHz data sets from both surveys reveal a predominant, relatively low, uniform backscatter return. As the operating frequency decreases, the circular patches of higher backscatter become visible in the 200 kHz and 100 kHz mosaics. This is particularly apparent in the 100 kHz mosaic (Figures 4 and 5), suggesting a frequency dependent response of the seafloor that is caused

by the surficial sediment characteristics. Fader and Miller [17] describe features in the Bedford Basin that are caused by disposal of dredge spoil, visible from sidescan sonar data, which are typically characterized by their circular shape and acoustically rough, high-backscatter surfaces, and that are often clustered together. They also describe the presence of biogenic gas within the soft sediments of the Bedford Basin, visible in seismic data sets. In some areas, these seismic data showed an absence of gas within the sediments that were directly beneath the deposited dredge spoil, where the spoil had disturbed and displaced the sediment and vented the gas. These descriptions are in agreement with the features described in our study from the multispectral multibeam data sets (Figure 4, Figure 5, and Figure 8).

Understanding the frequency dependent penetration into the substrate is complex, particularly from swath-acoustic remote sensing systems where acoustic grazing angle influences the way that the acoustic wave interacts with the seafloor. Backscatter intensity is a measure of the sound that is scattered back to the transducer by acoustic reflection and scattering [18]. Although there is generally a correlation between the measurable sediment characteristics and backscatter intensity [19,20], the relationship is very complex, with many variables that affect the backscatter intensity, which together describe the complex seafloor that exists in an environment [21]. Many of these variables that affect the seafloor acoustic response have been studied and modelled in both field and laboratory trials, the results from which allow us to deduce some general conclusions from our current multispectral backscatter study in the Bedford Basin.

The measured backscatter intensity is affected by interactions of the sound wave at the sediment-water interface (interface scattering) and from within the substrata (volume scattering) [22]. Both volume scattering and interface scattering are controlled by differences in impedance, which is a product of density and sound velocity [23]. Thus, in general, fine sediments, such as muds, tend to have higher porosity and therefore lower density and sound speed and they usually exhibit lower backscatter. In contrast, coarser sediments have lower porosity and higher density and sound speed, and therefore higher backscatter [22]. Relationships between these various parameters have been modelled in a number of studies (at frequencies <100 kHz), and they have demonstrated that volume scattering tends to be more important in determining the backscatter intensity in muddy substrata, whereas the bottom roughness was sufficient in explaining backscattering in sandy substrata [24,25]. This is also complicated by angular range, where grazing angle of the signal across the MBES swath affects the way that the sound interacts with the seafloor surface and subsurface characteristics [22,26]. Other parameters can also affect the backscatter intensity, such as the presence of gas in the sediment [15,27], bioturbation and presence of infauna [16,28], and sediment stratification [29]. When combined, these variables can all significantly complicate the relationship between backscatter intensity and seafloor environmental characteristics.

The acoustic frequency will also influence the way that the sound interacts with the seafloor [29,30]. The surface roughness of the sediment can affect the backscatter intensity that is based on the wavelength of the signal and the scale of roughness at the seafloor (e.g., surface roughness that is caused by grain size through to bedforms) [22]. The sediment parameters at the site can influence backscatter based on local roughness, which is often unknown or unmeasured [31], which in turn can cause different backscatter responses at different frequencies [16]. Generally speaking, lower frequency signals will penetrate deeper into the substrate than higher frequency signals, which will attenuate over a shorter distance [22,32].

Based on these earlier theoretical and empirical high frequency seafloor acoustic studies, we can deduce, from our study, that the lower-frequency 200 and 100 kHz signals are penetrating through the fine-grained, modern deposits at the seafloor surface of the Bedford Basin (characterized by the uniform, low backscatter intensities of the 400 kHz returns) to reveal the dredge spoil deposits (as described by Fader and Miller [17]), just below which have been smothered by more recent sedimentation events. Approximately 200 of these features have been identified, covering approximately 5% of the deep basin floor [17], which are very similar in appearance to the features that are visible in the 100 and

200 kHz multispectral MBES mosaics (Figures 4 and 5). The operating frequency of the sidescan sonar system that was used to collect the data described by Fader and Miller [17] was a dual-frequency Klein 100 and 320 kHz towfish. Fader and Miller [17] do not state the frequency of the sonograms at which the imaged dredge spoil was visible, but at lower operating frequency, we can speculate that they were also detecting sub-surface dredge spoil.

The characterization of these sediment-smothered, dredge spoil features from the multispectral backscatter is also corroborated by a comparison of the three multispectral mosaics with the underwater imagery data. Over most of the deeper-water regions of the study site the imagery revealed a seafloor comprised of soft mud, colonized by various soft sediment biota (e.g., burrowing anemones, polychaete worms, etc.) (Figure 6). This corresponds with the uniform low backscatter returns of the 400 kHz mosaic, but not the patches of higher backscatter that is attributed to the dredge spoil that was visible in the 100 and 200 kHz mosaics—confirming that these features are smothered in softer sediments. In contrast, at the entrance to the Narrows, the seafloor comprised a mixture of coarse substrata (bedrock, boulders, and cobbles with attached epifauna) (Figure 6 and Table 1). The backscatter in this region aligned more closely between the three multispectral mosaics, as would be expected in coarse, consolidated substrata, where signal penetration would be very limited and dominated by surface interface scatter.

Core penetration depths, both on and off the higher backscatter features in the lower frequency mosaics, also support the conclusion that the features visible in the lower-frequency mosaics are a result of the dredge spoil deposits beneath a surface of soft mud. Core penetration was greatly reduced on these high backscatter, 100 kHz and 200 kHz targets (<12 cm), as compared against core penetration depth in adjacent areas (>23 cm) where all three frequency mosaics showed uniform low intensity backscatter returns (Table 3). The grain size properties of the seafloor affect the core penetration depth. Reduced depth of penetration suggests that the corer was impeded by coarser-grained substrata below the mud at the seafloor surface. Although there was no evidence of the presence of coarse sediments following grain size analysis of the core samples, the corer would not be expected to sample these grain sizes due to the mechanics of the sampler. The presence of gas in the sediments, as also reported by Fader and Miller [17] in the Bedford Basin, could be another reason for the higher backscatter features in the lower frequency mosaics [15,27]. However, the presence of gas in the sediments would not impede core penetration, and biogenic gas would not likely occur in discrete circular features, such as the ones sampled.

The van veen grab samples also support this conclusion. The maximum penetration of the grab sampler was 20 cm, and the majority of the grab sample stations comprised >90% mud collected at the seafloor surface (Figure 7 and Table 2). However, sample station 016 comprised coarse sediments (11% gravel) and it coincided with one of the circular low-frequency high backscatter features (Figure 7), indicating that, at this location, the dredge spoil was close enough to the surface for the grab sampler to collect. Therefore, we can deduce that the 400 kHz backscatter signal is predominantly caused from the nominal interface scattering intensity for the water-sediment interface, and that the signal attenuates before reaching the subsurface dredge spoil. Any signal returned from this lower coarse sediment interface (e.g., where the dredge spoil is close enough to the surface of the seabed for the 400 kHz signal to reach) is either weaker than the intensity of the sea surface interface scatter or the volume scatter of the overlying mud, and therefore the features are not detected in the backscatter mosaic. In contrast, the 200 kHz and 100 kHz signals are penetrating through the surface mud and the scatter from the dredge spoil is higher than the overlying softer sediment. Therefore, these features are visible in the lower-frequency mosaics as local areas of high backscatter.

Comparison of the three multispectral mosaics along a transect from the mouth of the Bedford Basin to the deep water in the centre of the basin, traversing the dredge spoil features, also indicates the penetration differences attributed to the frequency response of the transmit signal (Figure 9). Hard substrata and regions of deep soft sediment deposits display similar changes in backscatter intensity along the transect for all three frequencies. The intensities diverge where hard deposits of

material are present below soft, surface sediments, with intensities increasing for the 100 and 200 kHz mosaics, but remaining consistently low for the 400 kHz mosaic (e.g., for the feature 250 m along the transect—Figure 9). These patterns are consistent in both the 2016 and 2017 data sets. The difference in absolute backscatter values between the 2016 and 2017 data sets when comparing each corresponding frequency is attributed to the uncalibrated nature of the backscatter from the MBES systems, which is a widely acknowledged issue when comparing the backscatter between systems (different R2Sonic 2026 units were used in the 2016 and 2017 surveys) [11,33].

5. Conclusions

The development of multibeam echosounder systems with multispectral backscatter capabilities is an exciting and innovative opportunity to improve the way that we map seafloor geology and benthic habitat. The results from this study have demonstrated the benefits that such a system can offer for improved understanding of seafloor geological characteristics. The intermittent ping cycle of the R2Sonic multispectral MBES provides backscatter at multiple frequencies from a single pass of the survey platform. This ability offers significant advantages, as it allows the same patch of seafloor to be imaged very close to the same grazing angle (i.e., nadir from one ping is nadir from an adjacent ping, and therefore all the imaging geometries for each frequency are co-located for every part of the survey area). A comparison of backscatter intensities between the frequencies is therefore possible without the complication of different ensonification angles. In comparison, studies that have collected multispectral backscatter data from multiple passes of a survey platform operating at a single frequency each time, even when closely following the same survey track on each pass, have difficulty in the precise co-location of ensonification geometries, which can complicate the comparison between frequencies. One possible downside of the intermittent ping cycle when operating in multispectral mode is that the along-track data resolution is lower when compared with operating in single-frequency mode (e.g., only one in three pings are used in the resulting mosaics—Figure 3). However, in our study, the sampling rate of the sonar was high enough to counter the along-track reduction in data density, and we did not notice any loss in the resolvability of seafloor features when compared against single frequency MBES backscatter mosaics that were collected at similar survey speeds from the same area [14].

There are many ways in which these data sets can be processed to generate seafloor thematic maps (Figure 1), and this is an ongoing and active field of research [6,7,34]. Combining multiple frequencies from multispectral MBES data in habitat mapping studies offers potential opportunities for improved discrimination of habitats. Many recent benthic habitat mapping studies are applying satellite remote sensing classification methods to objectively segment multibeam sonar data within GIS software using a combination of backscatter (monochromatic) and terrain attributes [35–37]. Several studies have gone further and have used species distribution modelling approaches to predict habitat suitability for target species with a great deal of success [35,38,39]. In such scenarios, defining the ecological niche of the target species that are based on terrain features and substrate characteristics is the key to success. The application of multispectral backscatter in such studies may offer significant advantages, particularly for soft sediment biota, where differences in signal penetration and volume scattering response change by frequency. However, to date, there are only a few examples of studies that have analyzed multispectral MBES backscatter data to segment and classify the seafloor [13,16,40,41]. The lack of research in this area has been mainly due to technology limitations, as up until recently MBES systems could not collect multiple frequencies in one pass of the survey vessel. Careful selection of the best combination of frequencies will be required to optimize the approach, and success will likely depend on site specific environmental characteristics. There is still much research that is needed in this field, with further testing and validation of the methodology required. However, the benefits of this approach to seafloor geological and habitat mapping are potentially ground-breaking in this field of study.

Author Contributions: Conceptualization, C.J.B., J.B. and M.B.; methodology, C.J.B., J.B. and M.B.; software, J.B.; validation, C.J.B. and V.G.; formal analysis, C.J.B., J.B., M.B. and V.G.; resources, C.J.B.; writing—original draft preparation, C.J.B., J.B. and M.B.; writing—review and editing, C.J.B., J.B., M.B. and V.G.; visualization, V.G.; supervision, C.J.B.; project administration, C.J.B.; funding acquisition, C.J.B.

Funding: This research was funded by through NSERC grant CIRC472115–14.

Acknowledgments: The authors would like to thank: Jason Hines and John Fulmer for support in MBES data analysis; Stephane Kirchhoff, Brittany Curtis, Jillian Ejdrygiewicz and Aaron Bishop for support in field operations and analysis of the video data. Chris Algar and Laura deGelleke for provision of grain size analysis from the sediment cores, and for use of the Dalhousie University multicore; Candace Smith (NSCC) and Tom Weber (University of New Hampshire) for review and discussion and advice on acoustic sediment interactions.

Conflicts of Interest: The authors declare no conflict of interest.

References

1. Ehler, C.; Douvère, F. Marine spatial planning: A step-by-step approach toward ecosystem-based management. In *Intergovernmental Oceanographic Commission and Man and the Biosphere Programme; IOC Manual and Guides No. 53, ICAM Dossier No. 6*; UNESCO: Paris, France, 2009. (In English)
2. Franklin, J. *Mapping Species Distributions*; Cambridge University Press: Cambridge, UK, 2009; p. 320.
3. Lu, D.; Weng, Q. A survey of image classification methods and techniques for improving classification performance. *Int. J. Remote Sens.* **2007**, *28*, 823–870. [[CrossRef](#)]
4. Lecours, V.; Devillers, R.; Schneider, D.C.; Lucieer, V.L.; Brown, C.J.; Edinger, E.N. Spatial Scale and Geographic Context in Benthic Habitat Mapping: Review and Future Directions. *Mar. Ecol. Prog. Ser.* **2015**, *535*, 259–284. [[CrossRef](#)]
5. Brown, C.J. Benthic Habitat Mapping: From backscatter to biology. *J. Ocean Technol.* **2015**, *10*, 48–61.
6. Brown, C.J.; Smith, S.J.; Lawton, P.; Anderson, J.T. Benthic habitat mapping: A review of progress towards improved understanding of the spatial ecology of the seafloor using acoustic techniques. *Estuar. Coast. Shelf Sci.* **2011**, *92*, 502–520. [[CrossRef](#)]
7. Diesing, M.; Green, S.L.; Stephens, D.; Lark, R.M.; Stewart, H.A.; Dove, D. Mapping seabed sediments: Comparison of manual, geostatistical, object-based image analysis and machine learning approaches. *Cont. Shelf Res.* **2014**, *8*, 107–119. [[CrossRef](#)]
8. Lecours, V.; Brown, C.J.; Devillers, R.; Lucieer, V.L.; Edinger, E.N. Comparing selections of environmental variables for ecological studies: A focus on terrain attributes. *PLoS ONE* **2016**. [[CrossRef](#)]
9. Lacharite, M.; Brown, C.J.; Gazzola, V. Multisource multibeam backscatter data: Developing a strategy for the production of benthic habitat maps using semi-automated seafloor classification methods. *Mar. Geophys. Res.* **2018**, *39*, 307–322. [[CrossRef](#)]
10. Boswarva, K.; Butters, A.; Fox, C.J.; Howe, J.A.; Narayanaswamy, B. Improving marine habitat mapping using high-resolution acoustic data; a predictive habitat map for the Firth of Lorn, Scotland. *Cont. Shelf Res.* **2018**, *168*, 39–47. [[CrossRef](#)]
11. Lurton, X.; Lamarche, G. (Eds.) Backscatter Measurements by Seafloor-Mapping Sonars. Guidelines and Recommendations. 2015. Available online: <http://geohab.org/wp-content/uploads/2014/05/BSWG-REPORT-MAY2015.pdf> (accessed on 15 January 2019).
12. Lamarche, G.; Lurton, X. Recommendations for improved and coherent acquisition and processing of backscatter data from seafloor-mapping sonars. *Mar. Geophys. Res.* **2018**, *39*, 5–22. [[CrossRef](#)]
13. Hughes Clarke, J.E. Multispectral Acoustic Backscatter from Multibeam, Improved Classification Potential. In Proceedings of the US Hydrographic Conference, National Harbor, MD, USA, 16–19 March 2015; p. 18.
14. Brown, C.J.; Smyth, S.; Furlong, A.; King, G.; Costello, G.; Potter, P.; Melton, J.S. A Synergistic Approach to improve Multibeam Backscatter Classification Methods for Geological/Habitat Mapping. In Proceedings of the Hydro 2010 Conference, Rostock-Warnemunde, Germany, 4 November 2010.
15. Schneider von Deimling, J.; Weinrebe, W.; Toth, Z.; Fossing, H.; Endler, R.; Rehder, G.; Spiess, V. A low frequency multibeam assessment: Spatial mapping of shallow gas by enhanced penetration and angular response anomaly. *Mar. Pet. Geol.* **2013**, *44*, 217–222. [[CrossRef](#)]
16. Feldens, P.; Schulze, I.; Papenmeier, S.; Schonke, M.; Schneider von Deimling, J. Improved Interpretation of Marine Sedimentary Environments Using Multi-Frequency Multibeam Backscatter Data. *Geosciences* **2018**, *8*, 214. [[CrossRef](#)]

17. Fader, G.B.J.; Miller, R.O. *Surficial geology, Halifax Harbour, Nova Scotia*; Geological Survey of Canada; Bulletin: Dartmouth, NS, Canada, 2008; Volume 590, p. 163.
18. Lurton, X. *An Introduction to Underwater Acoustics: Principles and Applications*, 2nd ed.; Springer/Praxis Publishing: Berlin, Germany, 2010; p. 704.
19. Collier, J.; Brown, C.J. Correlation of sidescan backscatter with grain size distribution of surficial seabed sediments. *Mar. Geol.* **2005**, *214*, 431–449. [[CrossRef](#)]
20. McGonigle, C.; Collier, J.S. Interlinking backscatter, grain size and benthic community structure. *Estuar. Coast. Shelf Sci.* **2014**, *147*, 123–136. [[CrossRef](#)]
21. Ferrini, V.L.; Flood, R.D. The effects of fine-scale surface roughness and grain size on 300 kHz multibeam backscatter intensity in sandy marine sedimentary environments. *Mar. Geol.* **2006**, *228*, 153–172. [[CrossRef](#)]
22. Jackson, D.R.; Richardson, M.D. *High-Frequency Seafloor Acoustics*; Springer: New York, NY, USA, 2007; p. 616.
23. Hamilton, E.L. Compressional-wave attenuation in marine sediments. *Geophysics* **1972**, *37*, 620–646. [[CrossRef](#)]
24. Jackson, D.R.; Winebrenner, D.P.; Ishimaru, A. Application of the composite roughness model to high-frequency bottom backscattering. *J. Acoust. Soc. Am.* **1986**, *79*, 1410–1422. [[CrossRef](#)]
25. Jackson, D.R.; Briggs, K.B. High-frequency bottom backscattering: Roughness versus sediment volume scattering. *J. Acoust. Soc. Am.* **1992**, *92*, 962–977. [[CrossRef](#)]
26. Aleshin, V.; Guillon, L. Modeling of acoustic penetration into sandy sediments: Physical and geometrical aspects. *J. Acoust. Soc. Am.* **2009**, *126*, 2206–2214. [[CrossRef](#)]
27. Fonseca, L.; Mayer, L.; Orange, D.; Driscoll, N. The highfrequency backscattering angular response of gassy sediments: Model/data comparison from the Eel River margin, California. *J. Acoust. Soc. Am.* **2002**, *111*, 2621–2631. [[CrossRef](#)]
28. Urgeles, R.; Locat, J.; Schmitt, T.; Hughes Clarke, J.E. The July 1996 food deposit in the Saguenay Fjord, Quebec, Canada: Implications for sources of spatial and temporal backscatter variations. *Mar. Geol.* **2002**, *184*, 41–60. [[CrossRef](#)]
29. Williams, K.L.; Jackson, D.R.; Tang, D.; Briggs, K.B.; Thorsos, E.I. Acoustic Backscattering From a Sand and a Sand/Mud Environment: Experiments and Data/Model Comparisons. *IEEE J. Ocean. Eng.* **2009**, *34*, 388–398. [[CrossRef](#)]
30. Williams, K.L.; Jackson, D.R.; Thorsos, E.I.; Tang, D.; Briggs, K.B. Acoustic Backscattering Experiments in a Well Characterized Sand Sediment: Data/Model Comparisons Using Sediment Fluid and Biot Models. *IEEE J. Ocean. Eng.* **2002**, *27*, 376–387. [[CrossRef](#)]
31. Lyons, A.P.; Pouliquen, E. Advances in high-resolution seafloor characterization in support of high-frequency underwater acoustics studies: Techniques and examples. *Meas. Sci. Technol.* **2004**, *15*, R59–R72. [[CrossRef](#)]
32. Schneider von Deimling, J.; Held, P.; Feldens, P.; Wilken, D. Effects of using inclined parametric echosounding on sub-bottom acoustic imaging and advances in buried object detection. *Geo Mar. Lett.* **2016**, *36*, 113–119. [[CrossRef](#)]
33. Malik, M.; Lurton, X.; Mayer, L. A framework to quantify uncertainties of seafloor backscatter from swath mapping echosounders. *Mar. Geophys. Res.* **2018**, *39*, 151–168. [[CrossRef](#)]
34. Ierodiaconou DSchimel, A.C.G.; Kennedy DMonk, J.; Gaylard, G.; Young, M.; Diesing, M.; Rattray, A. Combining pixel and object based image analysis of ultra-high resolution multibeam bathymetry and backscatter for habitat mapping in shallow marine waters. *Mar. Geophys. Res.* **2018**, *39*, 271–288. [[CrossRef](#)]
35. Brown, C.J.; Sameoto, J.A.; Smith, S.J. Multiple methods, maps and management applications: Purpose made seafloor maps in support of Ocean Management. *J. Sea Res.* **2012**, *7*, 1–13. [[CrossRef](#)]
36. Lucieer, V.; Hill, N.A.; Barrett, N.S.; Nichol, S. Do marine substrates ‘look’ and ‘sound’ the same? Supervised classification of multibeam acoustic data using autonomous underwater vehicle images. *Estuar. Coast. Shelf Sci.* **2013**, *117*, 94–106. [[CrossRef](#)]
37. Diesing, M.; Mitchell, P.; Stephens, D. Image-based seabed classification: What can we learn from terrestrial remote sensing? *ICES J. Mar. Sci.* **2016**, *73*, 2425–2441. [[CrossRef](#)]
38. Rengstorf, A.M.; Yesson, C.; Brown, C.; Grehan, A.J. Highresolution habitat suitability modelling can improve conservation of vulnerable marine ecosystems in the deep sea. *J. Biogeogr.* **2013**, *40*, 1702–1714. [[CrossRef](#)]
39. Young, M.A.; Ierodiaconou, D.; Edmunds, M.; Hulands, L.; Schimel, A.C.G. Accounting for habitat and seafloor structure characteristics on southern rock lobster *Jasus edwardsii*, assessment in a small marine reserve. *Mar. Biol.* **2016**, *163*, 141. [[CrossRef](#)]

40. Gaida, T.C.; Ali, T.A.T.; Snellen, M.; Amiri-Simkooei, A.; van Dijk, T.A.G.P.; Simons, D.G. A Multispectral Bayesian Classification Method for Increased Acoustic Discrimination of Seabed Sediments Using Multi-Frequency Multibeam Backscatter Data. *Geosciences* **2018**, *8*, 455. [[CrossRef](#)]
41. Janowski, L.; Trzcinska, K.; Tegowski, J.; Kruss, A.; Rucinska-Zjadacz, M.; Pocwiardowski, P. Nearshore Benthic Habitat Mapping Based on Multi-Frequency, Multibeam Echosounder Data Using a Combined Object-Based Approach: A Case Study from the Rowy Site in the Southern Baltic Sea. *Remote Sens.* **2018**, *10*, 1983. [[CrossRef](#)]



© 2019 by the authors. Licensee MDPI, Basel, Switzerland. This article is an open access article distributed under the terms and conditions of the Creative Commons Attribution (CC BY) license (<http://creativecommons.org/licenses/by/4.0/>).